RSC Advances

ROYAL SOCIETY OF CHEMISTRY

www.rsc.org/advances

Journal Name

ARTICLE

Soft amphiphilic polyesters obtained from PEGs and silicon fatty compounds: structural characterizations and self-assembly studies

Received 00th January 20xx,
Accepted 00th January 20xx

DOI: 10.1039/x0xx00000x

www.rsc.org/

Daniela Andrade[a], Claudio Moya[a], Felipe Olate[a], Nicolás Gatica[b], Susana Sanchez[b], Enzo Díaz[a], Elizabeth Elgueta[c], María Parra[a], Mohamed Dahrouch[a,] *

Transesterification polymerizations between a silicon fatty ester derived from methyl 10-undecenoate and polyethylene glycol (PEG) monomers generate amphiphilic biopolyesters with maximum molecular weights within two hours of reaction. The characterization of these products by FT-IR, ^{1}H NMR and ^{13}C NMR spectroscopies confirmed that these structures result from ester formation. These biopolyesters demonstrated thermal stability at temperatures higher than 400°C, with an increase in the heat of fusion (ΔH_{fus}) and melting temperature (Tm) as the PEGs' molecular weight increased. Self-assembly studies in water through fluorescence and TEM techniques revealed micelle formation, with a low critical aggregation concentration, for biopolyesters that incorporated PEGs with a molecular weight between 1000 and 3000 g/mol. The micelle sizes, determined via dynamic light scattering analysis, increased with the PEG length, with diameters between 70 and 190 nm. Fibre materials were prepared from biopolyesters containing PEGs with molecular weights higher than 1500 g/mol and were studied via polarizing optical microscopy.

Introduction

Polyethylene glycols (PEGs), also known as polyethylene oxides (PEOs), are compounds used in numerous daily applications[1]. For example, they are present in skin creams, toothpastes, lubricants, soft capsules, film coatings and excipients of pharmaceutical products. Their chemical and biological properties largely explain this broad range of applications[1-5]: PEG compounds are soluble in water as a result of the formation of hydrogen bonds with ether groups; they are nontoxic, and they present an excellent biocompatibility.

In the research field, the association of PEGs with active molecules is a growing research topic[4-18], particularly in studies aiming to obtain biomaterials while conserving some PEG properties, such as water-solubility and the hydrophilic behaviour[5, 19-24]. Most of the studies are in the area of biomedical sciences and are oriented to the use of these biomaterials as carriers for drug delivery[5, 6, 20, 21, 23]. The hydroxyl groups of PEG offer the possibility of covalent binding to drug molecules that could be posteriorly released via a chemical bond rupture; therefore, PEGs can be used as a carrier with different releasing mechanisms. However, it has been demonstrated that a more promising way to deliver drugs is the use of amphiphilic polymers[5, 21, 23], with PEGs as the hydrophilic block, bound to a molecular group with hydrophobic characteristics. Such materials could adopt a self-assembly structure[4, 19-25] with "micelle or vesicle" shapes in an aqueous solution, allowing them to carry and protect drug compounds, which must show good affinity for the hydrophobic block. If these amphiphilic polymers are designed for biological applications, it is desirable that the hydrophobic group is biocompatible and nontoxic [5, 20, 21, 23]. Moreover, the monomers carrying the hydrophobic groups must possess the ability to polymerize with PEG. Thus, to obtain amphiphilic materials based on PEGs with good probability for use in drug delivery applications, the focus of the experimental design should be on the adequate selection of hydrophobic monomers.

Biomass is currently considered a promising green alternative raw material[26-29], and a substantial amount of research is focused on the use of chemically modified triglycerides and fatty compounds from vegetable oils[30-32] as monomers in the polymer synthesis. Thus, polyamides, polyurethanes and polyesters[26, 30, 33, 34] can be easily prepared, showing similar properties to those obtained from petrochemical monomers. Because of their chemical characteristics, the products originating from fatty compounds[27] are usually classified as soft materials, with potential applications as liquid crystals, gels, fibres and carriers for drug delivery. Methyl 10-

[a] Departamento de Química Orgánica, Facultad de Ciencias Químicas, Universidad de Concepción, Casilla 160-C, Concepción, Chile. *E-mail: mdahrouch@udec.cl
[b] Departamento de Polímeros, Facultad de Ciencias Químicas, Universidad de Concepción, Casilla 160-C, Concepción, Chile.
[c] Centro de Investigación de Polímeros Avanzados (CIPA), Universidad de Concepción, Casilla 160-C, Concepción, Chile.

†Electronic Supplementary Information (ESI) available: thermogravimetric data of the monomers and the polyesters are given in the ESI. See DOI: 10.1039/x0xx00000x

undecenoate is one of these fatty monomers; it is derived from castor oil and has been used in different polymerization reactions[35]. Monomers, such as methyl 10-undecenoate, can show hydrophobic properties that are retained by the final polymer. The most important challenge in the preparation of these polymers is the chemical modification of fatty compounds to obtain monomers that are able to polymerize. In the case of methyl 10-undecenoate, the presence of the alkene and ester function allows for numerous chemical modifications. To preserve the hydrophobic character of methyl 10-undecenoate, Rivière and collaborators reported polyhydrosilylation reactions[36-39] of the alkene function when incorporating siloxane groups, which are known for their hydrophobicity, biocompatibility and thermal resistance properties. These silylated biomacromolecules have been shown to be biocompatible surfactants[38] and could adopt the micelle structure in organic solvents such as ethanol and heptane[36, 39]. The combination of PEG monomers with these silylated fatty esters, through polymerization reaction, should lead to soft polymers that are able to self-assemble in water.

The synthesis of novel amphiphilic polyesters, which include PEGs as a hydrophilic block and silylated fatty di-esters as a hydrophobic block, will be discussed in this article. The polyesterification reactions will be followed by molecular weight measurements using gel permeation chromatography techniques. Spectroscopy analyses (NMR and IR) will be used to determine the molecular structures. Thermal properties will be studied via thermogravimetric analysis (TGA) and differential scanning calorimetry (DSC). The micellar self-assembly of these materials in water will be followed by fluorescence measurements of pyrene in the hydrophobic region. Additionally, dynamic light scattering and electronic microscopy will show the formation of nano-biomaterials. These novel amphiphilic polyesters can also assemble as fibres and will be described and analysed via polarizing optical microscopy (POM).

Experimental

Materials. Poly(ethylene oxide) glycols of different molecular weights (Mn: 400, 1000, 1500, 2000 and 3000 g/mol), titanium-tetrabutoxide Ti(O-Bu)$_4$ and solvents were acquired from Aldrich and employed without any additional purification. The di-ester monomer H_3CO_2C-$(CH_2)_{10}$-$Si(CH_3)_2$-O-$Si(CH_3)_2$-$(CH_2)_{10}$-$CO2CH_3$, represented as MeOOC-FASi-COOMe, was synthesized according to a previously published procedure[39].

Characterization Techniques.

^{1}H NMR and ^{13}C NMR spectra were recorded using a Bruker Avance 400 MHz spectrometer, with $CDCl_3$ as the solvent and tetramethylsilane as an internal standard. FT-IR spectra were recorded using a Nicolet Magna 550 spectrophotometer. Elemental analyses were conducted using a Perkin-Elmer 240C elemental analyser.

Gel permeation chromatography (GPC) was performed using a Perkin Elmer Series 200 instrument at 20°C with a refraction index detector. All runs were performed with tetrahydrofuran (THF) as the eluent at a flow rate of 0.5 mL/min. A molecular weight calibration curve was obtained with poly(styrene) standards in the molecular weight range of 580 to 3,200,000 g/mol. The number average (M_n) and weight average (M_w) molecular weights were evaluated from these measurements.

Thermogravimetric (TG) measurements were conducted using a Netzsch TG209 F1 IRIS instrument in platinum pans at prescribed heating rates of 10°C/min in a range of 20°C to 500°C under a steady flow of nitrogen (20 mL/min).

Calorimetric behaviour was studied via DSC using a Netzsch DSC 204 F1 Phoenix differential scanning calorimeter. Samples (approximately 6-9 mg) were placed inside aluminium pans and heated under flowing nitrogen at 20 mL/min, ranging from -50 to 300 °C, at a 20 °C/min heating rate. With the aim to minimize differences in the thermal history of the samples, the corresponding thermograms were obtained, considering decomposition temperatures detected in TGA, according to the following temperature program: heating from -50 °C up to 300 °C (dynamic stage), isothermal stage at 300 °C (static), cooling until -50 °C (dynamic, quenching step), isothermal stage at -50 °C (static) and heating up to 300 °C (dynamic).

The critical aggregation concentration (CAC) value of the polyesters PE was achieved via steady-state fluorescence spectroscopy using pyrene as the fluorescent probe. A saturated aqueous solution of pyrene was used to prepare solutions of polyesters (Pes) from 0.001 to 0.1 [mg/mL]. Excitation spectra of pyrene were acquired using a Photon Technology International Inc. QuantaMaster fluorescence spectrometer in the range of 300 to 370 [nm], with an emission wavelength of 383 [nm]. The CAC of each PE was obtained from a plot of fluorescence intensity ratio 337/334 [nm] versus the logarithm of polyester PE concentration.

Transmission electron microscopy (TEM) was carried out using a JEOL 1200EXII instrument with an activation voltage of 120 kV. For sample preparation, a drop of each polymer solution was placed on a carbon-coated copper grid, followed by staining with 2% (w/v) uranyl acetate solution and drying at room temperature. The hydrodynamic diameter of the micellar particles was obtained via dynamic light scattering (DLS) using a Brookhaven 90Plus instrument. A 35 mW laser was applied at 532 nm, and the Stokes-Einstein equation was used to determine diffusion coefficients.

Fibrous textures were determined via POM (polarizing optical microscopy) using an Olympus BX51 optical microscope equipped with an Olympus U-TV0.5XC-3 polarizer and a LinkamT95-PE hot stage.

Synthesis of PE compounds.

The same methodology was used for the preparation of all polyesters, applying the same chemical route. The nomenclature used to name the different polyesters (PEs) starts with the molecular weight of the starting poly(ethylene oxide) glycol, followed by the polymerization time: for example, PE400-1 corresponds to the polyester coming from poly(ethylene oxide) glycol with a molecular weight (Mn) of 400 g/mol and is obtained after one hour of polymerization.

Methodology for polyester preparation: Poly(ethylene oxide) glycol (0.94 mmol) and $Ti(OBu)_4$ (0.03 mmol) were added to the di-ester monomer H_3CO_2C-$(CH_2)_{10}$-$Si(CH_3)_2$-O-$Si(CH_3)_2$-$(CH_2)_{10}$-CO_2CH_3 (0.94 mmol) under stirring. The mixture was heated to 140°C, and the pressure was reduced to 0.5 mmHg. When the temperature reached 190°C, it was maintained at this value, and the polymerization time started at this moment. Series of polyesters were obtained with polymerization times (PTs) of 1, 2 and 3 hours. After polymerization, the crude product was cooled and washed with 10 mL of pentane. After filtration and drying, all polyesters of the PE-1000, PE-1500, PE-2000 and PE-3000 series were obtained as white gummy solids, whereas the PE-400 series showed a liquid viscous aspect. Their respective yields are indicated in table 1.

Table 1 Reactions yields of the PEs

Polyesters	PE-400	PE-1000	PE-1500	PE-2000	PE-3000
Yield (%)	78	75	72	76	74

The representation of the polyester structures is given in figure 1:

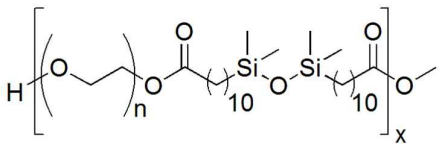

Fig. 1 Structural representation of the PEs

a) Characterization of compound PE400-2 (n=9)

FT-IR (KBr) cm^{-1}: 3506 (OH end group), 2922-2860 (Csp^3-H), 1736 (C=O), 1113 (C-O). ^{1}H-NMR ($CDCl_3$): δ 0.04 (s, 12H, Si-CH_3), 0.07 (s, 4H, Si-CH_2-), 0.51-1.63 (m, 32H, -CH_2-), 2.34 (t, 4H, O-CO-C**H$_2$**-), 3.67 (m, 36H, OCH_2CH_2O). ^{13}C-NMR ($CDCl_3$): δ 0.0 (Si-CH_3), 18.2 (-CH_2-Si), 23.1, 24.8, 29.1, 29.2, 29.3, 29.5, 29.6, 33.6, 34.1 (-$(CH_2)_9$-), 63.1 (O-CH_2-**C**H_2-O-CO-), 69.9 (O**C**H_2**C**H_2O), 173.3 (C=O), 61.7, 68.9, 72.5 (HO-**C**H_2-**C**H_2-O-, O-**C**H_2-CH_2-O-CO-). Elemental analysis data (%) for $(C_{44}H_{88}O_{13}Si_2)_m$, calculated: C 60.00, H 10.00; found: C 59.55, H 10.37.

b) Characterization of compound PE1000-2 (n=22)

FT-IR (KBr) cm^{-1}: 3450 (OH end group), 2922-2863 (Csp^3-H), 1735 (C=O), 1111 (C-O). ^{1}H-NMR ($CDCl_3$): δ 0.00 (s, 12H, Si-CH_3), 0.04 (s, 4H, Si-CH_2-), 0.46-1.58 (m, 32H, -CH_2-), 2.27 (t, 4H, O-CO-C**H$_2$**-), 3.61 (m, 88H, OCH_2CH_2O). ^{13}C-NMR ($CDCl_3$): δ 0.4 (Si-CH_3), 18.4 (-CH_2-Si), 23.3, 24.9, 29.0, 29.2, 29.3, 29.4, 29.6, 33.5, 34.2 (-$(CH_2)_9$-), 63.3 (O-CH_2-**C**H_2-O-CO-), 70.6 (O**C**H_2**C**H_2O), 173.4 (C=O), 61.7, 69.1, 72.7 (HO-**C**H_2-**C**H_2-O-, O-**C**H_2-CH_2-O-CO-). Elemental analysis data (%) for $(C_{70}H_{140}O_{26}Si_2)_m$, calculated: C 57.85, H 9.64; found: C 57.11, H 9.94.

c) Characterization of compound PE1500-2 (n=34)

FT-IR (KBr) cm^{-1}: 3453 (OH end group), 2886 (Csp^3-H), 1737 (C=O), 1112 (C-O). ^{1}H-NMR ($CDCl_3$): δ 0.00 (s, 12H, Si-CH_3), 0.04 (s, 4H, Si-CH_2-), 0.46-1.59 (m, 32H, -CH_2-), 2.30 (t, 4H, O-CO-C**H$_2$**-), 3.62 (m, 136H, OCH_2CH_2O). ^{13}C-NMR ($CDCl_3$): δ 0.3 (Si-CH_3), 18.4 (-CH_2-Si), 23.3, 24.9, 29.2, 29.3, 29.4, 29.5, 29.6, 33.5, 34.2 (-$(CH_2)_9$-), 63.3 (O-CH2-**C**H2-O-CO-), 70.2 (O**C**H_2**C**H_2O), 173.4 (C=O), 61.6, 69.2, 72.8 (HO-**C**H_2-**C**H_2-O-, O-**C**H_2-CH_2-O-CO-). Elemental analysis data (%) for $(C_{94}H_{188}O_{38}Si_2)_m$, calculated: C 56.97, H 9.49; found: C 56.22, H 10.01.

d) Characterization of compound PE2000-2 (n=45)

FT-IR (KBr) cm^{-1}: 3451 (OH end group), 2887 (Csp^3-H), 1738 (C=O), 1111 (C-O). ^{1}H-NMR ($CDCl_3$): δ 0.00 (s, 12H, Si-CH_3), 0.03 (s, 4H, Si-CH_2-), 0.48-1.63 (m, 32H, -CH_2-), 2.33 (t, 4H, O-CO-C**H$_2$**-), 3.66 (m, 180H, OCH_2CH_2O). ^{13}C-NMR ($CDCl_3$): δ 0.3 (Si-CH_3), 18.3 (-CH_2-Si), 23.2, 24.8, 29.0, 29.1, 29.3, 29.4, 29.6, 33.4, 34.2 (-$(CH_2)_9$-), 63.2 (O-CH_2-**C**H_2-O-CO-), 70.5 (O**C**H_2**C**H_2O), 173.4 (C=O), 61.6, 69.1, 72.5 (HO-**C**H_2-**C**H_2-O-, O-**C**H_2-CH_2-O-CO-). Elemental analysis data (%) for $(C_{116}H_{232}O_{49}Si_2)_m$, calculated: C 56.49, H 9.42; found: C 55.98, H 10.07.

e) Characterization of compound PE3000-2 (n=68)

FT-IR (KBr) cm^{-1}: 3495 (OH end group), 2888 (Csp^3-H), 1739 (C=O), 1111 (C-O). ^{1}H-NMR ($CDCl_3$): δ 0.01 (s, 12H, Si-CH_3), 0.05 (s, 4H, Si-CH_2-), 0.47-1.58 (m, 32H, -CH_2-), 2.31 (t, 4H, O-CO-C**H$_2$**-), 3.63 (m, 272H, OCH_2CH_2O). ^{13}C-NMR ($CDCl_3$): δ 0.4 (Si-CH_3), 18.5 (-CH_2-Si), 23.4, 24.5, 29.0, 29.2, 29.3, 29.4, 29.5, 33.5, 34.3 (-$(CH_2)_9$-), 63.4 (O-CH_2-**C**H_2-O-CO-), 70.6 (O**C**H_2**C**H_2O), 173.6 (C=O), 61.7, 69.2, 72.7 (HO-**C**H_2-**C**H_2-O-, O-**C**H_2-CH_2-O-CO-). Elemental analysis data (%) for $(C_{162}H_{324}O_{72}Si_2)_m$, calculated: C 55.93, H 9.32; found: C 55.25, H 9.76.

Fibre Preparation

The polymer sample was placed on a glass plate and heated. Once the melting phase was reached, the plate was removed from the heater and a glass capillary was dipped into the melted phase. Afterwards, the glass capillary was pulled to form a fibre, which was deposited on a glass plate for further analysis.

Results and discussion

Synthesis of PEs.

The transesterification polymerization between the fatty acid methyl di-ester H_3CO_2C-$(CH_2)_{10}$-$Si(CH_3)_2$-O-$Si(CH_3)_2$-$(CH_2)_{10}$-CO_2CH_3, denoted as MeOOC-FASi-COOMe, and the pol(ethylene glycol) HO-PEO-OH of different molecular weights (in the range of 400 to 3000 g/mol), using titanium-tetrabutoxide as the catalyst, generated the polyesters PE400, PE1000, PE1500, PE2000 and PE3000 with good yields, as shown in table 1. The reaction conditions were similar to those reported previously[39]. Briefly, the temperature of the reactions was progressively increased from 20° to 200°C. Simultaneously, the pressure was decreased from atmospheric

pressure to 0.5 mBar to shift the equilibrium to the products formation by methanol distillation and to allow simultaneous increase of the molecular weight. The chemical equation corresponding to these reactions is shown in figure 2.

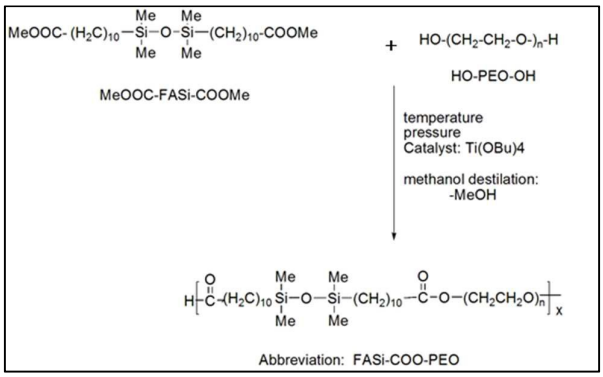

Fig. 2 Chemical equation of the transesterification polymerization reaction between the fatty acid methyl di-ester MeOOC-FASi-COOMe and the poly(ethylene glycol) HO-PEO-OH of different molecular weights.

Polymers with different molecular weights, determined via GPC (gel permeation chromatography), were obtained by changing and optimizing the times of the polymerization reaction (figure 3). Indeed, previous work[39-42] described that in the case of this polycondensation reaction and in the absence of solvent, an increase in miscibility between monomers substantially improved the molecular weights of the products. The poly(tetramethyleneglycol)s (PTMGs), which were investigated in the polymerization reaction with MeOOC-FASi-COOMe, lead to polymers with high molecular weights within only one hour of reaction due to their low polarity. Therefore, the polytransesterifcation reaction between the non-polar monomer MeOOC-FASi-COOMe and the polar monomer PEG should not easily lead to polymers with high molecular weights, which is usually related to materials with good thermal stability. The particularity of this polymerization reaction needs to be studied for various reaction times (1, 2 and 3 hours) to obtain a complete reaction and to achieve the highest molecular weights.

The physical aspects and solubility of these polyesters depend on the percentage of PEG incorporated into these materials. The PE400 series are viscous liquids and are soluble only in organic solvents, such as n-hexane, tetrahydrofuran, and chloroform, whereas the PE1000, PE1500, PE2000 and PE3000 series exhibit a gummy solid aspect and are soluble in water and polar organic solvents such as tetrahydrofuran and chloroform. The incorporation of PEG with higher molecular weights explains why these polyesters are soluble in water, i.e., hydrogen bonding. In comparison with the results reported previously[39], the similar polyesters based on PTMGs are not soluble in water because of the low hydrophilic characteristics exhibited by their respective monomers.

Gel permeation chromatography study.

Figure 3 shows the analysis of the gel permeation chromatography data. The variation of the molecular weight for the polyesters versus the polymerization time reached a maximum value after two hours, followed by a smooth decrease. Our interpretation of these results considers the fact that transesterification polymerization is a polycondensation reaction, where the monomers are added one by one to obtain the polymeric chain. Therefore, in this type of reaction, the difference in polarity between the monomers and their respective molecular weights is the most important factor that should be considered to explain these results. PEG monomers are hydrophilic, whereas the fatty acid methyl di-ester MeOOC-FASi-COOMe is hydrophobic. As the polymerization reaction proceeds, the polarity of the growing polymer changes, affecting the addition of the upcoming monomer. This resulting low miscibility between the reactants affects the interaction between the reacting groups, interfering with the growing of the polymer and leading to a decrease in the molecular weight. An opposite effect was observed[39] in the case of the polyesters obtained from PTMGs, as expected. Note that this polymerization reaction is carried out in the absence of solvent. No changes in molecular weight were expected after 2 hours of polymerization; however, a decrease in this parameter for all series was observed (figure 3). A possible explanation for this result may be related to the working temperature: at 200°C, thermal cracking of these polyesters may occur and induce the formation of oligomer fragments with lower molecular weight, such as those observed through gel permeation chromatography analysis. Because all of the GPC chromatograms present the same profiles and the same tendency, only one GPC chromatogram, corresponding to the PE1000 series, is shown in figure 3.

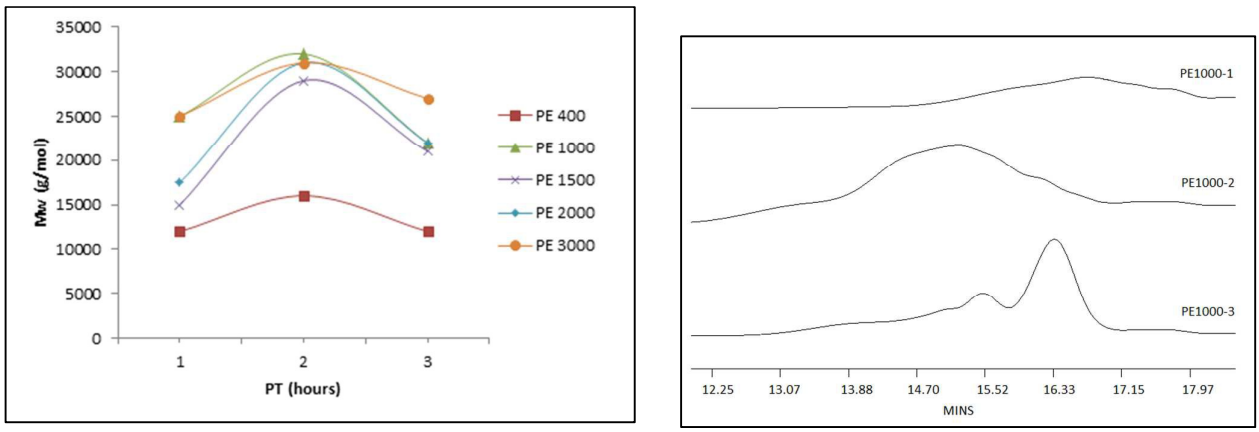

Fig. 3 Graph of molecular weight (Mw) versus polymerization time (PT) (left side); GPC chromatogram of polyester PE 1000 (right side).

As observed in figure 3, at any reaction time, no correlation was observed between the molecular weights of the PEG monomers and the growing polyesters. Therefore, instead of using the molecular weight parameter to compare the different polyesters, we used the degree of polymerization (Xw), as shown in table 2.

The largest value for the polymerization degree (Xw) was found for the polyesters PE400-2 and PE1000-2 (table 2). For the polyesters derived from PEG monomers 1500, 2000 and 3000, a significant drop in polymerization degree was observed and could be explained by the same reason mentioned previously, i.e., the concomitant increase in molecular weight and polarity of the PEG monomers decrease their miscibility with the hydrophobic MeOOC-FASi-COOMe monomer.

Table 2 Molecular weight of repeating unit (MU), Weight Average Molecular Weight (Mw), Number Average Molecular Weight (Mn), Weight Average Polymerization Degree (Xw), and Number Average Polymerization Degree (Xn).

Polyester	MU	Mw	Xw =Mw/MU	Mn	Xn =Mw/MU
PE400-2	900	15900	17.7	6800	7.6
PE1000-2	1500	31800	21.2	19300	12.9
PE1500-2	2000	28500	14.3	10500	5.3
PE2000-2	2500	31000	12.4	13000	5.2
PE3000-2	3500	31000	8.9	17300	4.9

Structural characterization of polyesters PE obtained after two hours of polymerization.

Characterization by FT-IR spectroscopy, ^{1}H and ^{13}C NMR and elemental analysis confirmed the structures of the synthetized polymers obtained after two hours of polymerization. The presence of a single absorption band near 1740 cm^{-1} in the FT-IR spectra was identified as the carbonyl function of the polyesters. Due to the good solubility of the polyesters in chloroform, NMR structural studies of these products were carried out in this solvent. The ^{1}H and ^{13}C NMR spectra showed chemical shifts different from those of the starting reagents (MeOOC-FASi-COOMe and PEG). Some of the most relevant information collected from the ^{13}C NMR spectra relied on the disappearance of the signal attributed to the carbon-methyl di-ester of the H_3**C**OOC-FASi-COO**C**H_3 monomer (53 ppm), confirming a total transesterification reaction. In all polyesters, the new signal observed near 63 ppm was assigned to the CH_2 group neighbouring the ester fragment, confirming the fatty ester incorporation in the polymer structure. These results are shown in an example of ^{13}C NMR spectra for PE-1000-2 in figure 4.

It is important to note that no significant difference in the yield and spectroscopic characterizations (FT-IR and RMN spectra) was observed for the polyesters obtained after 2 hours of polymerization.

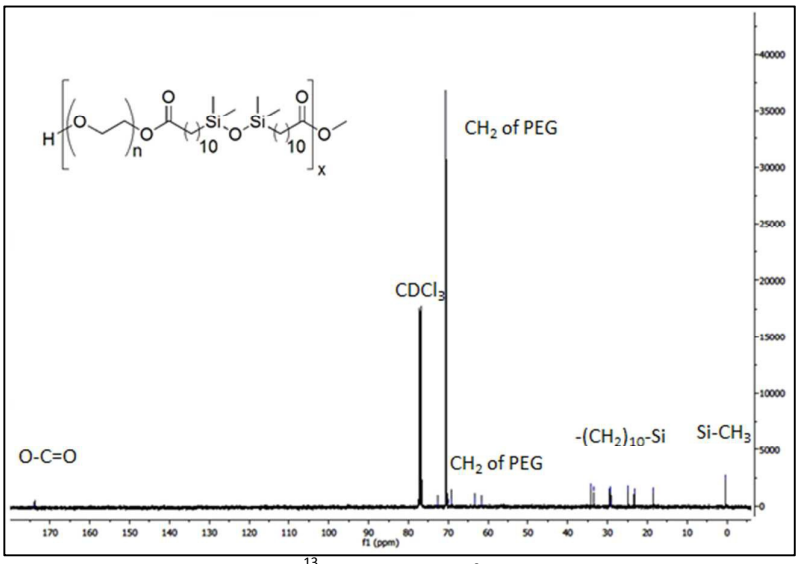

Fig. 4 ^{13}C NMR spectra of PE 1000-2

Thermal properties of Polyesters PE obtained after two hours of polymerization.

a) Thermogravimetric (TG) analyses

Thermogravimetric analyses were performed on polyesters PE400-2, PE1000-2, PE1500-2, PE2000-2 and PE3000-2, which exhibited the highest molecular weight. As representative examples, the thermal decomposition profiles of PE400-2 and PE1000-2 and the corresponding monomers are shown in figure 5. The polyesters PE1000-2, PE1500-2, PE2000-2 and PE3000-2 showed the same high thermal stability as the one presented by the PEG monomers and showed similar thermal decomposition curves with a unique mass loss (see supplementary information). The decomposition curves for PEG 400 and PE400-2 also indicate a unique mass loss; however, the thermal decomposition of the PEG 400 monomer was lower because of its minor molecular weight.

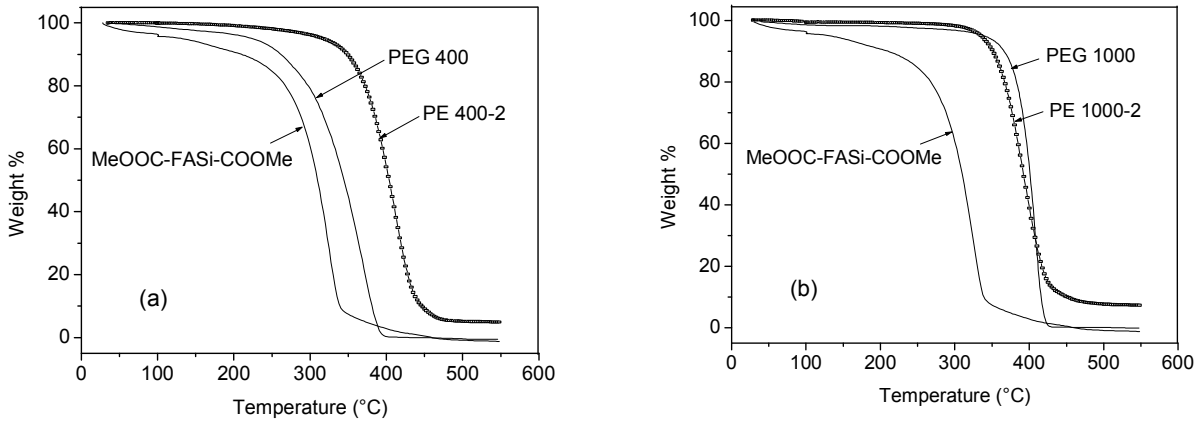

Fig. 5. Thermal decomposition profiles of: a) PE400-2, PEG 400 and MeOOC-FASi-COOMe and b) PE1000-2, PEG 1000 and MeOOC-FASi-COOMe.

These data indicate that incorporation of the fatty ester in PEG material did not disturb the PEG thermal properties and would enable these new polyesters to be used in applications that require high temperatures. A residual mass of approximately 5% is observed when the degradation of the polyesters is achieved at approximately 400°C. It is known that in reactions of organic-

inorganic hybrid materials with siloxane, the products obtained at high temperature are inorganic silica (SiO_2) and silicon oxycarbides (SiCxO4-x) due to the cleavage of Si-C and C-C bonds and the mineralization process[43, 44].

b) Differential scanning calorimeter (DSC) analysis

The Figure 6a shows the thermograms obtained for PE400-2, PE1000-2, PE1500-2, PE2000-2 and PE3000-2. Clear endothermic signals, representing polymer melting, can be observed in all cases. From these data, the heat of fusion (ΔH_{fus}) and melting temperature (Tm) values were determined (table 3). Both parameters, i.e., ΔH_{fus} and Tm, increased as the molecular weight of the polyesters increased from PE400-2 to PE3000-2. These results are consistent with an increase of the polymer crystallinity and the molecular weight of PEG: higher energy is needed to break the crystals of the new polymers as the chain length grows. In the case of a polar polymer or a polar macromolecular segment such as the PEG residues, there are more permanent dipoles in a longer chain[1]. Additionally, the high numbers of possible conformations, due to a high molecular weight, produce a high number of induced dipoles. Thus, dipolar interactions are involved between different chain segments, causing the formation of crystals and keeping them close.

The calorimetric behaviour, described previously, shows good agreement with the texture and solubility obtained for the polyesters synthesized: PE400-2 polyester is a viscous liquid soluble in n-hexane, whereas PE1000-2, PE1500-2, PE2000-2 and PE3000-2 polymers are gummy solid products soluble in water and ethanol. These observations can be considered as direct consequences of the higher polarity of the PEG segment as its molecular weight increases. To detect other transition processes for PE400, PE1000, PE1500, PE2000 and PE3000 polyesters and considering the size of melting signals, the corresponding thermograms were analysed between -50°C and 10 °C with an extended heat flow scale (figure 6b). Flat curves were obtained, and no glass transition peaks were observed between these temperatures. Glass transition is the result of molecular movements such as internal rotations and molecular sliding, which are eliminated with a low free volume. Macromolecular chains in the polyesters PE are close and packed, preventing the molecular movements. The absence of bulky side groups and the electronegative oxygen atoms present in the -$Si(Me)_2O$-, -COO- and $(-CH_2CH_2O-)_n$ groups would favour the intermolecular interactions and decrease the *free volume* of the polyesters chains.

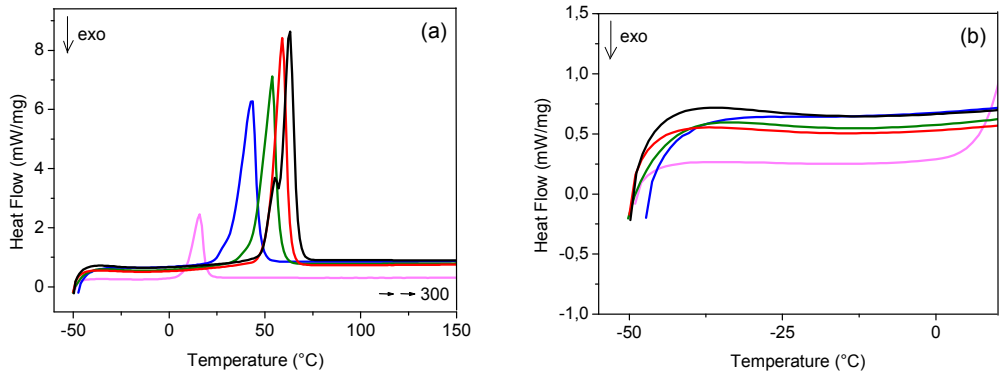

Fig. 6 Thermograms obtained via DSC of PE400-2 (—), PE1000-2 (—), PE1500-2 (—), PE2000-2 (—) and PE3000-2 (—) for a) temperature range between -50 °C and 150 °C and b) temperature range between -50 °C and -10 °C.

Table 3 Starting decomposition temperatures (SDT), heat of fusion (ΔH_{fus}), melting temperature (Tm), critical aggregation concentration (CAC) and particle size obtained by using DLS

Polymer	SDT (°C)	ΔH_{fus} (J/g)	Tm (°C)	CAC [mg/mL]	$Size_{(DLS)}$ (nm)
PE400-2	415	43.9	16.0	-	-
PE1000-2	401	166.9	43.2	0.0062	70
PE1500-2	400	167.7	53.9	0.0064	125
PE2000-2	403	171.9	59.1	0.0070	150
PE3000-2	402	194.1	62.8	0.0094	190

Micelle formation.

a) Fluorescence study

Because PE400-2 is insoluble in water, the study of micelle formation was performed only with PE1000-2, PE1500-2, PE2000-2 and PE3000-2 polyesters. A known methodology for studying the amphiphilic behaviour of polyesters consists of the incorporation of a fluorescent probe in the core of the micelles as they form[4, 45, 46]. Pyrene is a fluorescent dye usually used to show micelle formation[19, 36]. The CAC (critical aggregation concentration) for each polymer was determined using a pyrene ratio of excitation intensities at 337 and 334 [nm] (I337/I334) at an emission wavelength of 390 nm[19, 36]. As an example, the excitation spectrum of pyrene in solutions containing increasing concentrations of PE1000-2 is shown in figure 7a. As the polymer concentration increases, there is a shift from 334 nm to longer wavelengths. The polyesters PE1500-2, PE2000-2 and PE3000-2 exhibited similar behaviour. The CAC were determined from the plot of I337/I334 versus logarithm of polymer concentration (figure 7b) and are shown in table 3 for all analysed polymers. The CAC for the polyesters PE1000-2, PE1500-2, PE2000-2 and PE3000-2 were found to be in a range of 0.0062 to 0.0094 mg/mL, indicating that a low concentration of polymer was needed to form a micelle. PE1000-2, being the polyester with the highest content of hydrophobic group –FASi-, also showed the lowest CAC value. Indeed, previous reports[19, 47, 48] indicated that amphiphilic polymers having a large hydrophobic to hydrophilic block ratio showed a decreased CAC.

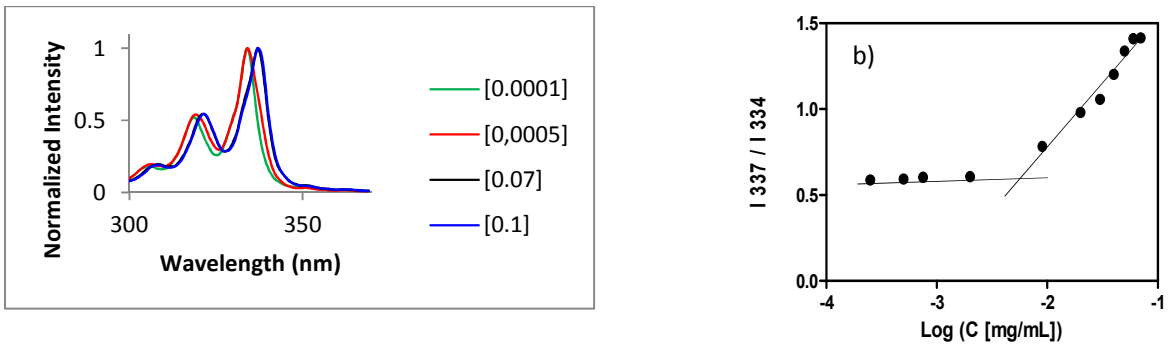

Fig. 7 a) Excitation spectra of a saturated aqueous solution of pyrene in the presence of PE1000-2 at different concentrations (mg /mL). b) Dependence of the intensity ratio (I_{337}/I_{334}) of pyrene on polymer PE1000-2 concentration [mg/mL].

b) Dynamic light scattering (DLS) and transmission electronic microscopies (TEM) analyses

To determine the sizes of the micelles, we used dynamic light scattering (DLS) and concentrations over the respective CAC for PE1000-2, PE-1500-2, PE2000-2 and PE3000-2. The results are shown in table 3. As expected, a clear relation between the molecular weight of the PEG segment and micelle size was observed: the increase in the micelle diameter was directly dependent on the PEG molecular weight. Because polymer conformation depends significantly on the polymer-solvent interactions, as the molecular weight of the PEG increases, the high

degree of intermolecular affinity between water and the hydrophilic PEG segments makes the polymer looser and more expanded, resulting in an increase in particle size. This behaviour is illustrated in figure 8. Additionally, note that the similar polyesters derived from PTMGs lead also to micelles with comparable size, despite the fact that they were obtained using a different solvent.

Transmission electronic microscopies (TEM) corroborate these results, showing clearly spherical aggregates corresponding to the micellar structures (figure 9). Note that similar TEM images have been reported in the literature[13, 39].

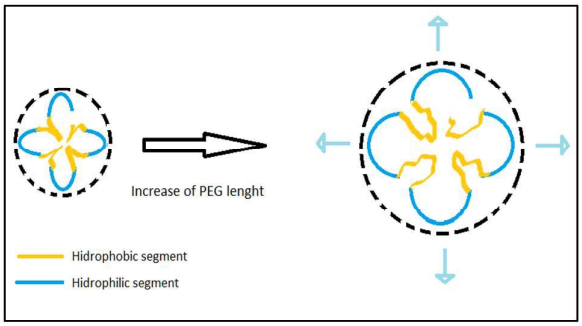

Fig. 8 Increase of micelle diameter with PEG length.

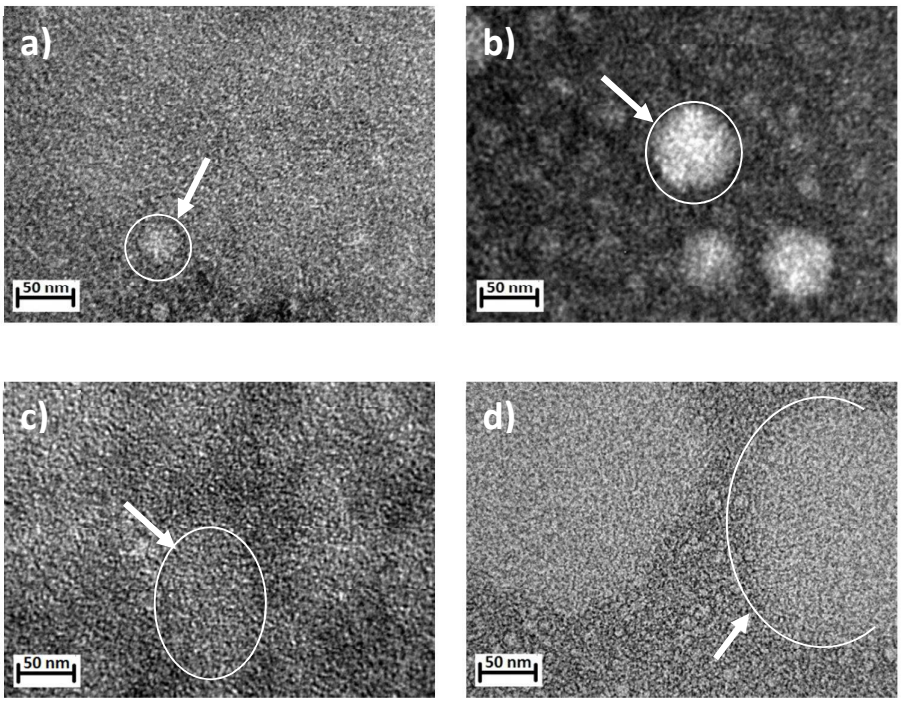

Fig. 9 TEM images of PE1000-2 (a), PE1500-2 (b), PE2000-2 (c) and PE3000-2 (d)

Preliminary results of fibre structure formation.

Amphiphilic polymers can also form fibres that could have several applications in tissue engineering[49-51]. Fibres were obtained using the PE1500-2, PE2000-2 and PE3000-2 series and applying the same process; their optical microscopy images are shown in figure 10. The low melting temperature (43°C) and crystallinity of the PE1000-2 polyester, as observed by DSC analysis, explain why no fibres were

formed from this polyester. PE2000-2 (figure 10c) and PE3000-2 (figure 10e) show fibres with uniform shape and diameters of 70 and 200 µm, respectively. However, in the case of PE1500-2 (figure 10a), the fibres formed were irregular in diameter and shape, likely due to a very low melting point. The thickness difference between the fibres obtained from PE2000-2 and PE3000-2 polyesters attracted our attention. The similar molecular weights of the polyesters PE2000-2 and PE3000-2could not be the factor that explains the differences in the thickness of the fibres. However, because the PEG length of the polyester PE3000-2 is longer than that of the polyester PE2000-2, the permanent dipoles should increase with increasing PEG length and should favour better packing.

The fibres were also observed via polarized light optical microscopy, with crossed polarizers of 90° (figure 10b, 10d and 10f). Spherulitic structures were identified, and we noticed that their size decreased considerably from the PE1500-2 fibre to the PE3000-2 fibre. According to the literature[52], this behaviour could be understood by considering that the PEG segment, presenting higher molecular weights, shows strong dipole-dipole interaction between the chains, leading to an increase of nucleation density and therefore a decrease in the spherulitic growth. Conversely, polymers with PEG units of lower molecular weight present weaker intermolecular interactions, allowing for folding behaviour of silicon fatty chains and favouring spherulitic growth through molecular self-assembly.

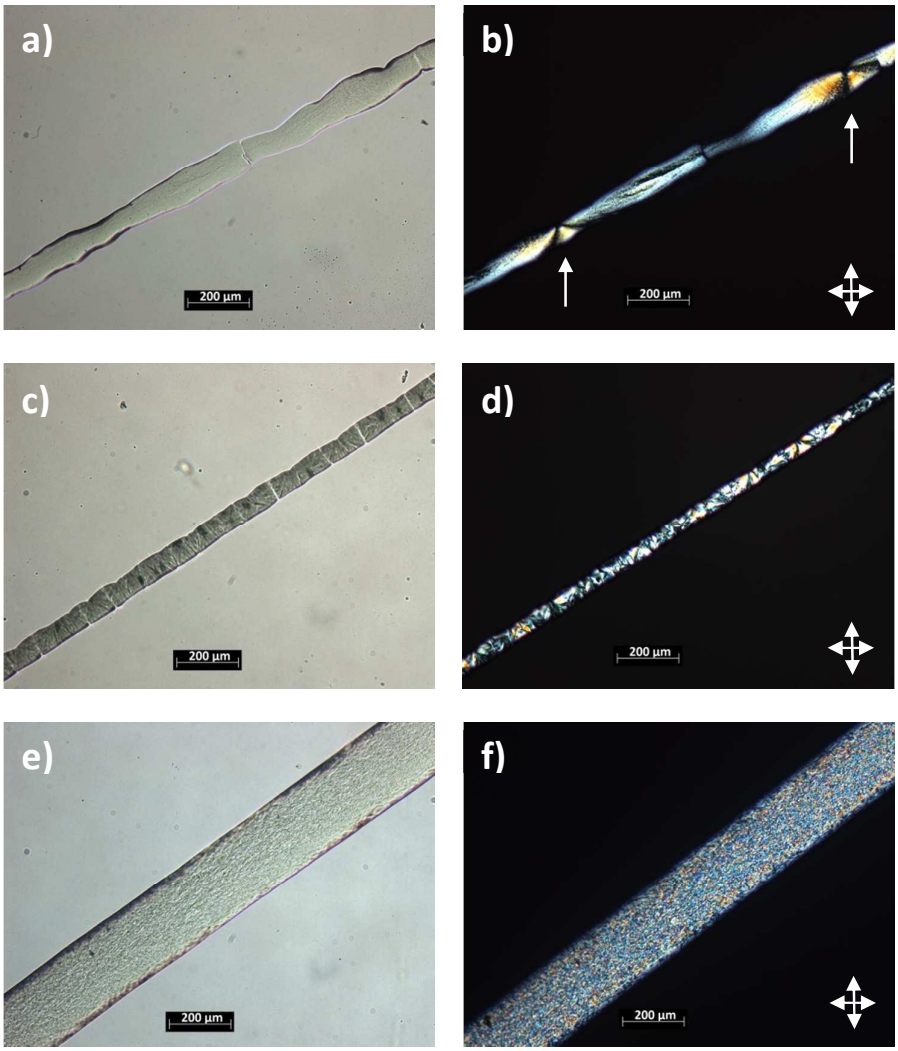

Fig. 10 Optical micrographs of fibres observed for optical microscopy under parallel (on the left) and crossed (on the right) polarizing of PE1500-2 (10a and 10b), PE-2000 (10c and 10d) and PE3000-2 (10e and 10f), respectively.

Conclusions

In spite of the extreme polarity difference present between the monomers, the transesterification reactions of PEGs with the silylated fatty di-ester were carried out successfully with a high degree of purity and allowed the synthesis of a very attractive class of amphiphilic polyesters using a renewable fatty ester derived from castor oil. Their preparation could easily be followed via spectroscopic analysis, confirming the expected structures. Contrary to the similar polyesters based on PTMGs, which showed self-assembly only in organic solvents, the self-assembling abilities of these novel polyesters obtained from PEGs lead to micelle structures in water, showing a hydrophobic fatty ester core surrounded by hydrophilic PEG groups. Such results were confirmed using fluorescence techniques, light scattering and microscopy. A potential application offered by these novel materials could be found in the field of drug delivery, where the presence of the fatty compound would provide excellent biocompatibility, promoting good interactions between micelle structures and cell membranes. It is important to underline that our synthesis methodology allows for obtaining different particle sizes depending on the PEG length, enabling the evaluation of changes in drug concentrations. Regarding drug release, perspectives of future work are oriented toward the investigation of micelle structure in an apolar environment and the study of partial hydrolysis in the ester functions present in these polymers. These polyesters also showed the ability to form fibres when their melting points were higher than 50°C. The thicknesses of the fibres could also be changed according to the PEG length. We consider our results to be very promising for the synthesis of biocompatible materials, and they encourage us to continue our research on biological applications, particularly regarding the release of active molecules. Additionally, the high thermal stability, observed until 400°C, enables an exciting application of these polyesters in research fields where this parameter may be crucial.

Acknowledgements

The authors thank the Project “Fondecyt 1130606” and the “Vice-Rectoría de Investigación” of Concepción University (Chile) for their financial support.

References

1. S. Zalipsky and J. M. Harris, in *Poly(Ethylene Glycol): Chemistry and Biological Applications*, eds. J. M. Harris and S. Zalipsky, Editon edn., 1997, vol. 680, pp. 1-13.
2. J. Nicolas, S. Mura, D. Brambilla, N. Mackiewicz and P. Couvreur, *Chemical Society Reviews*, 2013, **42**, 1147-1235.
3. D. Hutanu, M. D. Frishberg, L. Guo and C. C. Darie, *Modern Chemistry & Applications*, 2014, **2**, 132.
4. J. P. Jain, W. Y. Ayen and N. Kumar, *Current Pharmaceutical Design*, 2011, **17**, 65-79.
5. M. Barz, R. Luxenhofer, R. Zentel and M. J. Vicent, *Polymer Chemistry*, 2011, **2**, 1900-1918.
6. D. Gu, K. Ladewig, M. Klimak, D. Haylock, K. M. McLean, A. J. O'Connor and G. G. Qiao, *Polymer Chemistry*, 2015, **6**, 6475-6487.
7. A. Kolate, D. Baradia, S. Patil, I. Vhora, G. Kore and A. Misra, *Journal of Controlled Release*, 2014, **192**, 67-81.
8. I. W. Hamley, *Biomacromolecules*, 2014, **15**, 1543-1559.
9. K. Letchford, R. Liggins and H. Burt, *Journal of Pharmaceutical Sciences*, 2008, **97**, 1179-1190.
10. E. M. Pelegri-O'Day, E.-W. Lin and H. D. Maynard, *Journal of the American Chemical Society*, 2014, **136**, 14323-14332.
11. U. P. Shinde, H. J. Moon, D. Y. Ko, B. K. Jung and B. Jeong, *Biomacromolecules*, 2015, **16**, 1461-1469.
12. Y. Ding, P. Zhang, X.-Y. Tang, C. Zhang, S. Ding, H. Ye, Q.-L. Ding, W.-B. Shen and Q.-N. Ping, *Polymer*, 2012, **53**, 1694-1702.
13. B. Obermeier and H. Frey, *Bioconjugate Chemistry*, 2011, **22**, 436-444.
14. F. Wurm, J. Klos, H. J. Raeder and H. Frey, *Journal of the American Chemical Society*, 2009, **131**, 7954-+.
15. J. Lee, M. K. Joo, H. Oh, Y. S. Sohn and B. Jeong, *Polymer*, 2006, **47**, 3760-3766.
16. C. Mangold, F. Wurm, B. Obermeier and H. Frey, *Macromolecules*, 2010, **43**, 8511-8518.
17. W. Tian, J. Liu, Y. Guo, Y. Shen, D. Zhou and S. Guo, *Journal of Materials Chemistry B*, 2015, **3**, 1204-1207.
18. L. Wang, J. Wang, X. Gao, Z. Liang, B. Zhu, L. Zhu and Y. Xu, *Polymer Chemistry*, 2014, **5**, 2836-2842.
19. Q. Cui, F. Wu and E. Wang, *Journal of Physical Chemistry B*, 2011, **115**, 5913-5922.
20. M. L. Lopez-Donaire, E. M. Sussman, M. Fernandez-Gutierrez, A. Mendez-Vilas, B. D. Ratner, B. Vazquez-Lasa and J. San Roman, *Biomacromolecules*, 2012, **13**, 624-635.
21. A. Z. Samuel and S. Ramakrishnan, *Macromolecules*, 2012, **45**, 2348-2358.
22. G. B. H. Chua, P. J. Roth, H. T. T. Duong, T. P. Davis and A. B. Lowe, *Macromolecules*, 2012, **45**, 1362-1374.
23. S. Ma, Y. Hu and R. Wang, *Macromolecules*, 2015, **48**, 3112-3120.
24. B. Reid, S. Tzeng, A. Warren, K. Kozielski and J. Elisseeff, *Macromolecules*, 2010, **43**, 9588-9590.
25. S.-C. Chen, L.-L. Li, H. Wang, G. Wu and Y.-Z. Wang, *Polymer Chemistry*, 2012, **3**, 1231-1238.
26. A. Corma, S. Iborra and A. Velty, *Chemical Reviews*, 2007, **107**, 2411-2502.
27. P. K. Vemula and G. John, *Accounts of Chemical Research*, 2008, **41**, 769-782.
28. K. K. Bansal, D. Kakde, L. Purdie, D. J. Irvine, S. M. Howdle, G. Mantovani and C. Alexander, *Polymer Chemistry*, 2015, **6**, 7196-7210.
29. F. H. Isikgor and C. R. Becer, *Polymer Chemistry*, 2015, **6**, 4497-4559.

30. U. Biermann, U. Bornscheuer, M. A. R. Meier, J. O. Metzger and H. J. Schaefer, *Angewandte Chemie-International Edition*, 2011, **50**, 3854-3871.
31. M.-H. Alves, H. Sfeir, J.-F. Tranchant, E. Gombart, G. Sagorin, S. Caillol, L. Billon and M. Save, *Biomacromolecules*, 2014, **15**, 242-251.
32. F. Stempfle, D. Quinzler, I. Heckler and S. Mecking, *Macromolecules*, 2011, **44**, 4159-4166.
33. Y. Lu and R. C. Larock, *Chemsuschem*, 2009, **2**, 136-147.
34. J. Hong, Q. Luo, X. Wan, Z. S. Petrovic and B. K. Shah, *Biomacromolecules*, 2012, **13**, 261-266.
35. T. Lebarbe, L. Maisonneuve, N. Thi Hang Nga, B. Gadenne, C. Alfos and H. Cramail, *Polymer Chemistry*, 2012, **3**, 2842-2851.
36. A. El Kadib, N. Katir, N. Marcotte, K. Molvinger, A. Castel, P. Riviere and D. Brunel, *Journal of Materials Chemistry*, 2009, **19**, 6004-6014.
37. A. El Kadib, N. Katir, A. Castel, F. Delpech and P. Riviere, *Applied Organometallic Chemistry*, 2007, **21**, 590-594.
38. F. Delpech, S. Asgatay, A. Castel, P. Riviere, M. Riviere-Baudet, A. Amin-Alami and J. Manriquez, *Applied Organometallic Chemistry*, 2001, **15**, 626-634.
39. N. Katir, A. El Kadib, M. Dahrouch, A. Castel, N. Gatica, Z. Benmaarouf and P. Riviere, *Biomacromolecules*, 2009, **10**, 850-857.
40. M. Jose Climent, A. Corma, S. B. A. Hamid, S. Iborra and M. Mifsud, *Green Chemistry*, 2006, **8**, 524-532.
41. M. Jayakannan and S. Ramakrishnan, *Macromolecular Rapid Communications*, 2001, **22**, 1463-1473.
42. M. Dahrouch, A. Schmidt, L. Leemans, H. Linssen and H. Gotz, *Macromolecular Symposia*, 2003, **199**, 147-162.
43. V. Belot, R. J. P. Corriu, D. Leclercq, P. H. Mutin and A. Vioux, *Journal of Non-Crystalline Solids*, 1992, **147**, 52-55.
44. R. O. Pinho, E. Radovanovic, I. L. Torriani and I. V. P. Yoshida, *European Polymer Journal*, 2004, **40**, 615-622.
45. G. Yu, K. Jie and F. Huang, *Chemical Reviews*, 2015, **115**, 7240-7303.
46. J. S. Lee and J. Feijen, *Journal of Controlled Release*, 2012, **161**, 473-483.
47. L. Chen, T. Ci, L. Yu and J. Ding, *Macromolecules*, 2015, **48**, 3662-3671.
48. M. Ukawala, T. Rajyaguru, K. Chaudhari, A. S. Manjappa, S. Pimple, A. K. Babbar, R. Mathur, A. K. Mishra and R. S. R. Murthy, *Drug Delivery*, 2012, **19**, 155-167.
49. A. B. Kutikov and J. Song, *ACS Biomaterials Science & Engineering*, 2015, **1**, 463-480.
50. R. Langer and D. A. Tirrell, *Nature*, 2004, **428**, 487-492.
51. R. Langer and J. P. Vacanti, *Science*, 1993, **260**, 920-926.
52. Y. Li, Q. Ma, C. Huang and G. Liu, *Materials Science-Medziagotyra*, 2013, **19**, 147-151.

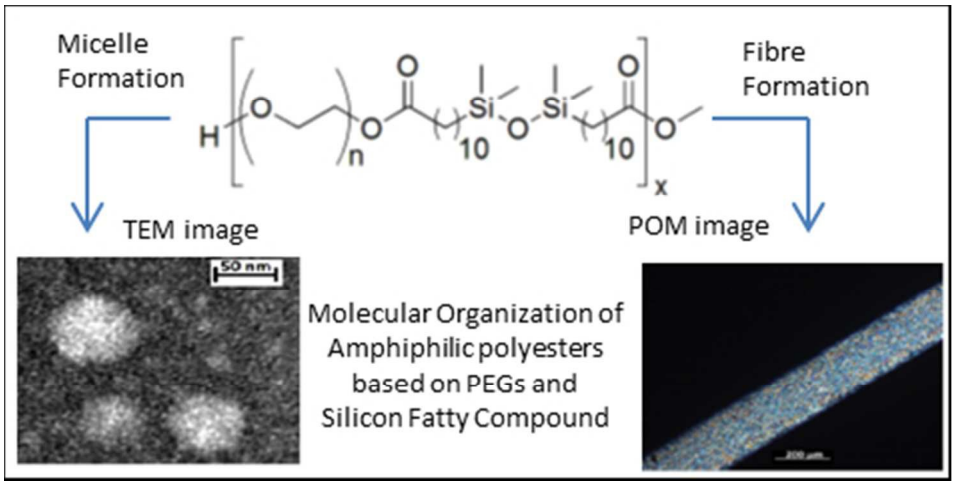

80x40mm (150 x 150 DPI)